



# THE UNIVERSITY *of* EDINBURGH

## Edinburgh Research Explorer

### How accurately should we model ice shelf melt rates?

**Citation for published version:**

Goldberg, D, Gourmelen, N, Snow, K, Kimura, S & Millan, R 2018, 'How accurately should we model ice shelf melt rates?' *Geophysical Research Letters*. DOI: 10.1029/2018GL080383

**Digital Object Identifier (DOI):**

[10.1029/2018GL080383](https://doi.org/10.1029/2018GL080383)

**Link:**

[Link to publication record in Edinburgh Research Explorer](#)

**Document Version:**

Peer reviewed version

**Published In:**

*Geophysical Research Letters*

**General rights**

Copyright for the publications made accessible via the Edinburgh Research Explorer is retained by the author(s) and / or other copyright owners and it is a condition of accessing these publications that users recognise and abide by the legal requirements associated with these rights.

**Take down policy**

The University of Edinburgh has made every reasonable effort to ensure that Edinburgh Research Explorer content complies with UK legislation. If you believe that the public display of this file breaches copyright please contact [openaccess@ed.ac.uk](mailto:openaccess@ed.ac.uk) providing details, and we will remove access to the work immediately and investigate your claim.



# How accurately should we model ice shelf melt rates?

D. N. Goldberg,<sup>1</sup>N. Gourmelen, <sup>1</sup>S. Kimura, <sup>2</sup>R. Millan <sup>3</sup>, K. Snow <sup>4</sup>

<sup>1</sup>School of Geosciences, University of Edinburgh, Edinburgh, United Kingdom

<sup>2</sup>JAMSTEC, Japan

<sup>3</sup>U. California-Irvine, United States

<sup>4</sup>Australia National University, Canberra, Australia

## Key Points:

- Satellite measurement of melt rates shows high spatial variability under two fast-flowing ice shelves
- Ice-sheet response to ice shelf melt depends on the pattern of melt rates as well as their spatial average
- The ability of an ocean model to reproduce this pattern depends on accurate bathymetry and ice shelf draft data

## Abstract

Assessment of ocean-forced ice sheet loss requires that ocean models be able to represent sub-ice shelf melt rates. However, spatial accuracy of modelled melt is not well investigated, and neither is the level of accuracy required to assess ice sheet loss. Focusing on a fast-thinning region of West Antarctica, we calculate spatially resolved ice-shelf melt from satellite altimetry, and compare against results from an ocean model with varying representations of cavity geometry and ocean physics. Then, we use an ice-flow model to assess the impact of the results on grounded ice. We find that a number of factors influence model-data agreement of melt rates, with bathymetry being the leading factor; but this agreement is only important in isolated regions under the ice shelves, such as shear margins and grounding lines. To improve ice sheet forecasts, both modelling and observations of ice-ocean interactions must be improved in these critical regions.

## 1 Introduction

In certain locations along the Antarctic coastline [Arneborg *et al.*, 2012; Dutrieux *et al.*, 2014; Greenbaum *et al.*, 2015], warm Circumpolar Deep Water (CDW) exists on the continental shelf as a result of Ekman upwelling, weaker sea ice growth and deep oceanic troughs [Jenkins *et al.*, 2016; Walker *et al.*, 2013; Petty *et al.*, 2013], leading to high ice-shelf basal melt rates. In recent years, this melt has led to a large reduction in ice-shelf mass, particularly in the Amundsen Sea region [Pritchard *et al.*, 2012; Paolo *et al.*, 2015]. This reduction lessens buttressing of the ice sheet, increasing ice sheets' contribution to sea levels [Thomas, 1979; Shepherd *et al.*, 2004; Jacobs *et al.*, 2012; Joughin *et al.*, 2014].

Estimates of melt rates under Amundsen ice shelves have typically been area-averaged or area-integrated; either because estimates are based on hydrographic measurements [e.g., Jacobs *et al.*, 2011; Rignot *et al.*, 2013; Randall-Goodwin *et al.*, 2015; Miles *et al.*, 2016], or because the spacing of satellite altimetry tracks does not allow for spatially-resolved measurement [Pritchard *et al.*, 2012; Paolo *et al.*, 2015]. However, a number of studies have found spatially resolved measurements through high-resolution remote sensing methods [Dutrieux *et al.*, 2013; Berger *et al.*, 2017; Gourmelen *et al.*, 2017], showing that melt rates can differ widely from their areal average at spatial scales on the order of kilometers.

44           Meanwhile there has been a great deal of effort in the modelling of ice-ocean in-  
45           teractions in the Amundsen [e.g., *Payne et al.*, 2007; *Robertson*, 2013; *Dutrieux et al.*,  
46           2014; *St-Laurent et al.*, 2015; *Kimura et al.*, 2017; *Nakayama et al.*, 2017]. While regional  
47           ocean models have been successful in reproducing ocean circulation and its link to bulk  
48           ice-shelf melt, ice modelling suggest that the *location* of ice removal from an ice shelf,  
49           in addition to its bulk value, may impact its buttressing capacity [*Goldberg et al.*, 2012;  
50           *Goldberg and Heimbach*, 2013; *Seroussi et al.*, 2017; *Arthern and Williams*, 2017]. The  
51           extent to which ocean models reproduce this spatial variability is unclear, and there is  
52           a need to strengthen the link between ocean and ice modelling if assessments of ice-sheet  
53           response to ocean forcing are to be made.

54           In this study, we employ a high-resolution ocean model with newly derived bathy-  
55           metric data, validated against high-resolution satellite observations of melt, to better con-  
56           strain the spatial variations in ice-shelf melt rates and evaluate their effect on ice-sheet  
57           stability using an adjoint-modelling approach. Focussing on Dotson and Crosson ice shelves,  
58           both situated in the Amundsen Sea and subject to strong CDW forcing, we examine the  
59           effects of different representations of bathymetry, ice-shelf draft, and physics of the ice-  
60           ocean boundary layer upon both melt rates and impact to grounded ice. We find that  
61           a number of factors are important to reproducing the observed spatial melt variability;  
62           but that capturing this variability is more important in some locations than others, at  
63           least where ice-sheet response is of interest.

## 64           2 Study Area

65           Smith, Pope, and Kohler Glaciers are three narrow interconnected ice streams in  
66           the Amundsen sector of West Antarctica, which drain into Crosson and Dotson Ice shelves.  
67           For purpose of discussion we adopt terminology from *Khazendar et al.* [2016] and *Gourme-*  
68           *len et al.* [2017] and refer to them (in east-to-west order) as Pope, Smith, Kohler East,  
69           and Kohler West (Fig. 3(a)). Although their contribution to ice flux from the continent  
70           is  $\sim 7$ -8 times smaller than that of Thwaites and Pine Island Glaciers [*Shepherd et al.*,  
71           2002], their observed thinning rates are even larger than that of these bigger ice streams  
72           [*McMillan et al.*, 2014a]. They have exhibited significant grounding line retreat in re-  
73           cent years, with the Smith grounding line retreating at rates upward of  $2 \text{ km a}^{-1}$  [*Scheuchl*  
74           *et al.*, 2016]. Ice-sheet modelling suggests that this retreat may have been induced by  
75           a decrease in buttressing from the Crosson and Dotson Ice Shelves [*Goldberg et al.*, 2015],

76 consistent with observations of increased velocities close to the grounding line of these  
 77 ice streams [Mouginot *et al.*, 2014; Lilien *et al.*, 2018].

78 This drop in buttressing may be related to submarine melt-induced thinning, which  
 79 can decrease buttressing [e.g., Shepherd *et al.*, 2004]. High melt rates have been observed  
 80 for both Dotson and Crosson in recent years [Depoorter *et al.*, 2013; Rignot *et al.*, 2013;  
 81 Randall-Goodwin *et al.*, 2015; Miles *et al.*, 2016; Gourmelen *et al.*, 2017; Lilien *et al.*, 2018].  
 82 Between 2003-2008, Dotson and Crosson had net average thinning rates of 3.1 and 6.5  
 83 m a<sup>-1</sup>, respectively [Rignot *et al.*, 2013]; and both have had strong thinning trends for  
 84 the last two decades [Paolo *et al.*, 2015].

85 Previously, numerical modelling of ice-ocean interactions under these ice shelves  
 86 has been challenging due to inaccurate bathymetric information [Schodlok *et al.*, 2012].  
 87 A previous estimate of bathymetry, RTOPO [Timmermann *et al.*, 2010], was constructed  
 88 from a series of bathymetric soundings. However, the dataset contains little information  
 89 underneath Crosson and Dotson. A recent study [Millan *et al.*, 2017] used gravity data  
 90 from Operation IceBridge to generate a far more detailed bathymetric map of the region,  
 91 revealing a significant cavity beneath Crosson Ice Shelf as well as a substantial oceano-  
 92 graphic connection between Crosson and Dotson. The findings raise questions of whether  
 93 models require accurate bathymetry to assess oceanographic influence on ice sheets.

### 94 **3 Methods**

#### 95 **3.1 Melt rates from remote sensing**

96 We generate swath elevation of Dotson and Crosson from CryoSat-2 between 2010  
 97 and 2015 [Gourmelen *et al.*, 2018] and, to avoid interference of advecting ice-shelf topog-  
 98 raphy, solve for the Lagrangian rate of surface elevation change on a 500 by 500m grid  
 99 [Gourmelen *et al.*, 2017]. The Lagrangian rate of change is performed using Sentinel-1  
 100 derived velocities [McMillan *et al.*, 2014b]. The melt rate is assessed through the follow-  
 101 ing [Jenkins and Doake, 1991]:

$$m = \dot{a} - \frac{\dot{s} + s \nabla \cdot \mathbf{u}}{1 - \frac{\rho_i}{\rho_w}} \quad (1)$$

102 where  $m$  is basal melt rate,  $\dot{a}$  is the surface mass balance [van Wessem *et al.*, 2016],  $\rho_i$   
 103 is ice density of  $917 \text{ kg m}^{-3}$ ,  $\rho_w$  nominal ocean density of  $1028 \text{ kg m}^{-3}$ ,  $\mathbf{u}$  is ice veloc-  
 104 ity, and  $s$  is surface elevation from the DEM, corrected for a 1.5 m penetration bias.

### 105 3.2 Ocean cavity modelling

106 We use the Massachusetts Institute of Technology general circulation model (MIT-  
 107 gcm; Marshall *et al.* [1997]) to model the circulation and melt rates underneath Dotson  
 108 and Crosson Ice Shelves. The ocean model uses a stereographic polar projected grid and  
 109 is restricted to a small domain (Fig. 1) which includes the ice-shelf cavities. External  
 110 ocean boundary conditions are imposed from the output of a regional ocean simulation  
 111 of the Amundsen Sea and shelf break [Kimura *et al.*, 2017]. The Kimura simulation was  
 112 forced by atmospheric reanalysis and agrees well with available observations, and can  
 113 be considered a reliable product for conditions at our domain boundaries. Monthly av-  
 114 erages of temperature, salinity and velocity for 2010-2014 are interpolated to our domain  
 115 boundaries. The model is spun-up for 2 years with 2010 forcing. No sea-ice or ocean sur-  
 116 face forcing is included in the model.

117 Several different bathymetries and ice-shelf drafts are tested. We use RTOPO bathymetry  
 118 and draft for comparison with the Millan *et al.* [2017] bathymetry and draft – referred  
 119 to as the Millan bathymetry and draft. Additionally we use an ice-shelf draft calculated  
 120 from the CryoSat-derived DEM for the period 2010-2015, assuming hydrostatic floatation  
 121 and a uniform firn column air content of 17 m [Ligtenberg *et al.*, 2014] – referred  
 122 to as the CryoSat draft. (We note that the Millan ice-shelf draft is derived from BEDMAP2  
 123 ice-shelf surface elevation [Fretwell *et al.*, 2013].)

124 Sub-ice shelf melt rates are calculated with a viscous sublayer model, which param-  
 125 eterizes turbulent fluxes of heat and salt just beneath the ice [Losch, 2008]. These fluxes  
 126 are determined by turbulent exchange coefficients [Holland and Jenkins, 1999]. While  
 127 some studies assume constant exchange coefficients [e.g., Losch, 2008; Seroussi *et al.*, 2017],  
 128 MITgcm explicitly represents their dependency on near-ice velocities [Dansereau *et al.*,  
 129 2014]. We carry out simulations with both velocity-dependent and non-velocity depen-  
 130 dent parameterizations. In the velocity-dependent runs, the frictional drag coefficient  
 131  $c_D$  in the formulation

$$u_*^2 = c_D |\mathbf{U}|^2 \quad (2)$$

132 (where  $u_*^2$  is normalised interfacial drag, and  $\mathbf{U}$  is near-ice velocity) is chosen to give area-  
 133 average modelled melt similar to that of the observations for Dotson and Crosson. In  
 134 the non-velocity dependent run, the temperature exchange coefficient ( $\gamma_T$ ) is chosen to  
 135 achieve the same (with  $\gamma_S$ , the salt exchange coefficient, held to a fixed ratio). Exper-  
 136 iments are summarised in Table 1, and other relevant ocean model parameters are given  
 137 in Table S1 of the Supplement.

### 138 **3.3 Ice sheet-ice shelf modelling**

139 We use the STREAMICE ice flow package of MITgcm [*Goldberg and Heimbach,*  
 140 2013] to model the response and sensitivity of Smith, Pope and Kohler Glaciers to melt  
 141 rates under Dotson and Crosson. We use it as a standalone model, run in the domain  
 142 indicated in Fig. 1(a) with 450 m resolution, and a fixed time step of  $\frac{1}{24}$  years. BEDMAP2  
 143 data gives bathymetry and initial ice thickness. To address the lack of cavity data in BEDMAP2,  
 144 we artificially deepen the bed by 50% seaward of its grounding line. While our modifi-  
 145 cation of BEDMAP2 could bias against grounding line advance, the historic trend has  
 146 been one of thinning and retreat. Still, this highlights the need for more reliable topo-  
 147 graphic data sets that extend over the entire continent.

148 In order to assess sensitivities the model is calibrated to observations, i.e. a model  
 149 *inversion* is carried out. As described in the Section 2.2 of the Supplement, we constrain  
 150 the time-evolving model, which is forced by ocean-modelled melt, to MEaSURES (450  
 151 m) velocities [*Rignot et al., 2011*] as well as a record of grounded thinning rates [*Gourme-*  
 152 *len et al., 2018*]. Basal traction and Glen’s flow law coefficient [*Cuffey and Paterson, 2010*]  
 153 are used as controls – as in *Goldberg et al. [2015]*, grounded ice stiffness is determined  
 154 by estimating the thermal steady-state, and Glen’s law coefficient is adjusted only in float-  
 155 ing ice.

156 The number of control parameters is roughly  $2.5 \times 10^5$ , so to minimize model-data  
 157 misfit an adjoint approach is used [*MacAyeal, 1992*]. We use the Automatic Differen-  
 158 tiation tool OpenAD [*Utke et al., 2008*] which allows adjoint sensitivities of STREAM-  
 159 ICE to be generated easily in both time-independent and time-dependent modes [*Gold-*  
 160 *berg et al., 2016*].

161 Finally, calibrated parameters are used to initialise time-dependent model runs. The  
162 time-dependent adjoint model is used to assess sensitivity of grounded ice volume to melt  
163 rates over 15 years. We do not force our model with surface accumulation as we expect  
164 its low values in this region (30-40 cm per year, *Arthern et al.* [2006]) to have minimal  
165 dynamic impact over the time scale investigated; however, such forcing would be nec-  
166 essary for century-scale runs.

167 We stress that our use of thinning observations in our calibration is not meant to  
168 reproduce evolution of the system over a specific time window; rather, it is to initialise  
169 the model in a dynamic state representative of that of Smith, Pope and Kohler. The ice  
170 model, calibration and initialisation processes, and adjoint sensitivity calculation are ex-  
171 plained in more detail in the Supplement [*Goldberg, 2011; Pattyn et al., 2013; Fürst et al.,*  
172 *2015*].

## 173 4 Results

### 174 4.1 Remotely-sensed melt rates

175 The 2011-2015 average surface elevation of Dotson and Crosson Ice Shelves is shown  
176 in Fig. 1. The surface depression related to the channel discussed in *Gourmelen et al.*  
177 [2017] is clearly visible, as is another smaller, narrower depression just to the west. Crosson  
178 Ice Shelf has a number of linear features in its surface, including a long narrow depres-  
179 sion connecting the Smith grounding line to the tip of Bear Peninsula. This feature cor-  
180 responds to a region of strong localised shear in the velocity field (Fig. 3(a)).

181 Melt rates derived from our calculation of surface rate-of-change and advective pro-  
182 cesses are shown in Fig. 2(a). Again, a clear signal of the channelised melting from *Gourme-*  
183 *len et al.* [2017] can be seen. Other high-melting regions are near the Smith and Pope  
184 grounding lines, as well as an elongated region south of Bear Peninsula, just east of the  
185 Dotson-Crosson shear margin. Thinning is evident in this region from the altimetry (Fig  
186 S1, Supplement).

187 The results suggest little melt in the south-east portion of Crosson and even localised  
188 freezing. Freezing is likely an artefact of our lagrangian tracking, since Crosson is heav-  
189 ily rifted in these regions, and freezing is unlikely given nearby observed ocean temper-  
190 atures [*Randall-Goodwin et al., 2015; Jenkins et al., 2018*].



## 191 4.2 Modelled melt rates

192 Fig. 2(b-d) show melt rate results, averaged for each of the simulations over the  
 193 years 2011-2015. Area-average melt rates (separately for each ice shelf and combined)  
 194 are given in Table 1. For each model result, the average is over the region where there  
 195 is circulation beneath an ice shelf. For the satellite-derived melt rates, two values are found:  
 196 one in which rates are filtered between  $-100 \text{ ma}^{-1}$  and  $+100 \text{ ma}^{-1}$  (from examination  
 197 of outliers in a melt-rate distribution), and one between 0 and  $+100 \text{ ma}^{-1}$ . The latter  
 198 value assumes that the negative melt rates found are artefacts, and the ocean melt-rate  
 199 parameters  $c_D$  and  $\gamma_T$  are based on this value.

200 Both runs with the Millan bathymetry and velocity-dependent melt (Figs. 2(b,c))  
 201 show a channelised feature along the western margin of Dotson, similar to observations.  
 202 However, melt is elevated along the entire margin, in contrast to observations. It is worth  
 203 noting that elevated melt is indicated by the observations along the west margin, just  
 204 upstream of the grounding line protrusion. Thus it is possible that these two “tributaries”  
 205 of the channelised melt region are simply expressed in differing degrees by the model and  
 206 observations.

207 Melt rates with the CryoSat draft (Figs. 2(c,d)) have a similar pattern to obser-  
 208 vations along the western margin of Crosson, just south of Bear Peninsula. Here the mixed  
 209 layer is likely guided by inverted depressions in the ice shelf (Fig. S2, Supplement), while  
 210 Coriolis focuses the outflow on the margin. In contrast, the topography of the Millan draft  
 211 guides the flow northward (fig. 2(b)).

212 With a velocity-independent melt parameterisation (Fig. 2(d)), melt is actually de-  
 213 creased in the location of the channelised feature, and in Crosson’s west shear margin,  
 214 suggesting a velocity-driven mechanism in the channel. On the other hand, there is bet-  
 215 ter agreement with observations near the Pope, Smith, and Kohler East grounding lines.  
 216 (All models other than the RTOPO model indicate high melt near the Kohler West ground-  
 217 ing line.) The low melt rates near the grounding line in the velocity-dependent models  
 218 are due to low velocities just beneath the shelf. This is in line with idealised models us-  
 219 ing velocity-dependent melt rates [*Little et al.*, 2009; *Snow et al.*, 2017], which also sug-  
 220 gest low melting at the grounding line. The RTOPO model (see Fig. S3, Supplement)  
 221 does indicate elevated melt rates along Dotson’s west margin, but the poor agreement  
 222 in every other respect is likely due to the incorrect bathymetry.

223 The time series of melt shows a generally decreasing trend (Fig. S4, Supplement).  
 224 This is in line with oceanographic estimates [*Jenkins et al.*, 2018], although a temporary  
 225 increase in 2013 is seen. As our study focuses on melt rate patterns this is not detrimental  
 226 to our aims, but care should be taken when interpreting our modelled melt rate evolution.  
 227

### 228 4.3 Grounded ice sensitivity to melt rates

229 Adjoint sensitivities of *VAF* (Volume Above Floatation; *Dupont and Alley* [2005])  
 230 to melt rates are calculated for Dotson and Crosson Ice Shelves (Fig. 3(b)). Specifically  
 231 these are found with respect to a “control run” (*CONTROL*) forced with time-average  
 232 melt from Model 1, so chosen due to the close correspondence between the Millan draft  
 233 and the initial ice draft. *VAF* is used as it is a measure of potential contribution to sea  
 234 levels; but it is not the only measure of melt rate impact on grounded ice, as discussed  
 235 below.

236 Upon examining the adjoint sensitivities, some interesting patterns emerge. Sen-  
 237 sitivities are seen to be small over most of Dotson, aside from the grounding line of Kohler  
 238 West. Sensitivity is slightly elevated where channelised melt-driven thinning takes place,  
 239 but this is still small. On Crosson, sensitivities are largest in the vicinity of ice rumples  
 240 and along the Pope, Smith and Kohler East grounding lines. Of note, however, is the  
 241 high sensitivity along the velocity shear margin of Crosson where it borders Dotson and  
 242 the southern edge of Bear Peninsula. We note that the results are broadly similar to those  
 243 of *Reese et al.* [2018], who examined instantaneous velocity response of a time-independent  
 244 model to ice-shelf mass removal on a coarse grid.

245 The calculated adjoint sensitivities can be used to generate linearized responses of  
 246 *VAF* to different melt rate perturbations as follows. If  $m_i$  is the melt rate in an ocean  
 247 grid cell  $i$ , then the incremental *VAF* response (relative to that of the *CONTROL* ex-  
 248 periment) is found by

$$\Delta VAF = \sum_i (m_i - m_i^{ref}) \delta^* m_i, \quad (3)$$

249 i.e. a summation over all cells  $i$ , where  $m_i^{ref}$  is the melt rate from Model 1, and  $\delta^* m_i$   
 250 is the sensitivity of  $\Delta VAF$  to melt rate in the cell  $i$ :

$$\delta^* m_i = \frac{\partial(\Delta VAF)}{\partial m_i}, \quad (4)$$

251 evaluated at  $m^{ref}$ .

252 Eq. 3 is evaluated for each melt field (modelled and observed), with results given  
 253 in Table 1. Despite the observed melt pattern having a smaller spatial average than that  
 254 of Model 1, it yields a larger *VAF* loss. The reason can be traced to greater melt rates  
 255 near grounding lines, particularly Kohler West and Kohler East. Still, the ice-sheet im-  
 256 pact is relatively similar among the models (aside from the RTOPO model).

257 It is also informative to consider the melt rate pattern of “maximal impact” from  
 258 a grounded ice loss perspective – this is a melt rate perturbation which is an exact scal-  
 259 ing of melt rate sensitivities:

$$\Delta m_i^{max} = \left( \frac{nM}{\sum_i \delta^* m_i} \right) \delta^* m_i \quad (5)$$

260 where  $n$  is the total cell count, and  $M$  is a perturbation spatial average. Choosing  $M$   
 261 =  $3 \text{ ma}^{-1}$  (in line with the approximate thinning rate of both Crosson and Dotson over  
 262 the past two decades, *Paolo et al.* [2015]) leads to a linearly predicted *VAF* loss of  $32.1$   
 263  $\text{km}^3$ . For reference, a spatially uniform perturbation of  $3 \text{ ma}^{-1}$  yields predicted loss of  
 264  $8.6 \text{ km}^3$ .

265 The above are linear estimates – a limitation of the adjoint approach. For instance,  
 266 grounding line retreat leads to loss of backstress from basal traction and can lead to in-  
 267 creased grounding line thickness, which cannot be detected by linearising about a fixed  
 268 trajectory. We run two additional time-dependent simulations of the same length as *CONTROL*:  
 269 one in which melt rate is equal to  $(m^{ref} + \Delta m^{max})$ ; and one in which it is equal to  $(m^{ref} +$   
 270  $M)$ . The former is referred to as the *FOCUS* run below, while the latter is referred to  
 271 as *CONST*. The impact of the perturbations on thinning and ice speed relative to *CONTROL*  
 272 are shown in Figs. 3(c-f). *FOCUS* yields considerably higher grounded thinning of the  
 273 ice streams (up to  $70 \text{ m}$  over the modelled period in some locations), and also increased  
 274 grounded speeds (up to  $220 \text{ ma}^{-1}$ ), as well as considerable speedup of Crosson. The as-  
 275 sociated *VAF* losses in the *FOCUS* and *CONST* experiments are  $41.3$  and  $14.0 \text{ km}^3$   
 276  $\text{a}^{-1}$ , respectively. These are higher than the predicted linear responses, likely due to model  
 277 nonlinearities.

## 5 Discussion

In our experiments, the ocean simulation which gives the best agreement with observations in terms of reproducing large-scale features (Model 2) nonetheless underestimates melt in key areas such as grounding lines. The results raise questions as to the requirements of ocean cavity models to best predict future impacts of ocean forcing on Antarctica. If the most important aspect of the melt field is near the grounding line, then accurate bathymetry – which determines delivery of dense CDW – becomes crucial.

The importance of melt near the grounding line also highlights the importance of the ocean model’s melt-rate parameterisation. Although our velocity-independent melt model reproduces the high melt rates observed near the grounding line, this does not necessarily mean such a parameterisation is the correct one to use, as it could neglect important processes, such as potential accelerated melt due to runoff [Berger *et al.*, 2017; Smith *et al.*, 2017], or potential ice-shelf collapse due to channelised melt [Gourmelen *et al.*, 2017]. Furthermore, we do not represent tidal effects, which could potentially be important [Jourdain *et al.*, 2019]. Moreover, our analysis assumes the satellite-inferred melt rates to be “truth”, but the assumption of hydrostatic floatation could lead to systemic errors, particularly within  $\sim 5$  kilometers of the grounding line [Brunt *et al.*, 2010]. Thus, improved observations of melt rates in the vicinity of the grounding line are needed, as well as an improved representation of ocean physics in this critical region.

In our analysis, we have assumed submarine melting to be the primary driver of loss of grounded ice. However, there are other processes that can affect ice-shelf buttressing. Ice stiffness (the Glen’s law parameter) influences ice flow in a similar manner to thickness and ice-shelf weakening can have a similar effect to melt-induced thinning. In fact, Lilien *et al.* [2018] infer weakening of the Dotson-Crosson margin from 1996-2011. Adjoint sensitivity to Glen’s law parameter (not shown) has a pattern similar to that of melting, and it is possible that observed speedup of Smith, Pope and Kohler East is due to weakening in this shear margin. Alternatively, thinning in the western shear margin of Crosson could potentially be influencing and accelerating this weakening: as an ice shelf thins in its shear margin, shear stress and strain rates increase. Larger shearing stresses might then lead to higher levels of ice damage [Borstad *et al.*, 2016], and thus further weakening. If such a process were to continue indefinitely, it could lead to an effective separation of Crosson and Dotson ice shelves, as has been observed for Thwaites Ice Tongue

310 and Thwaites Eastern Ice Shelf – an event which has led to a large shift in the grounded  
311 velocity of Thwaites Glacier [*Mouginot et al.*, 2014].

312 The *FOCUS* ice model experiment leads to far more thinning and speedup than  
313 the *CONST* run. Still, the additional mass loss,  $\sim 3 \text{ km}^3 \text{ a}^{-1}$ , is not large relative to the  
314  $\sim 21 \text{ km}^3 \text{ a}^{-1}$  currently being lost from the region. Moreover there is little modelled ground-  
315 ing line retreat, despite extensive retreat observed [*Rignot et al.*, 2014]. The lack of ground-  
316 ing line retreat (which would lead to additional *VAF* loss) may be because the nature  
317 of the experiments precludes melt under newly floating ice; other modelling studies [*Seroussi*  
318 *et al.*, 2017; *Arthern and Williams*, 2017] suggest that melting of newly exposed shelf  
319 near the grounding line has a large impact on retreat. Additionally, the initial model ice  
320 thickness could be predisposed against retreat: BEDMAP thicknesses are much higher  
321 than initial thickness used in *Goldberg et al.* [2015] along most of the grounding line (Fig.  
322 S7, Supplement). That study produced large grounding line retreat using the same model  
323 at the same resolution. Thus our experiments show that melt pattern – and not just melt  
324 volume – can have an important impact on grounded ice; but other processes are required  
325 for extensive retreat.

## 326 6 Conclusions

327 By comparing high-resolution satellite-inferred observations of ice-shelf melt against  
328 ocean cavity models, we have shown that reasonable agreement can be achieved with suf-  
329 ficiently accurate boundary conditions such as ice-shelf draft and ocean bathymetry. How-  
330 ever, analysis of sensitivities of an ice sheet-ice shelf model suggests this agreement may  
331 only be important in certain locations, if the aim is to model and understand ice-sheet  
332 response to ocean forcing. Equivalently, melt rate patterns can be as important as bulk  
333 melt in determining grounded ice response to melt.

334 For small, narrow ice shelves like Crosson and Dotson, these locations of high sen-  
335 sitivity to melt are likely to include those near the grounding lines and regions of high  
336 shear. Thus it is very important that ocean models represent ice-ocean physics accurately  
337 in these critical locations. Moreover, it is important that observations of melt in these  
338 critical locations be improved – since without this, the veracity of ocean models in these  
339 locations, and hence their utility in predicting future ice-sheet response to climate vari-  
340 ability and change, cannot be assessed.

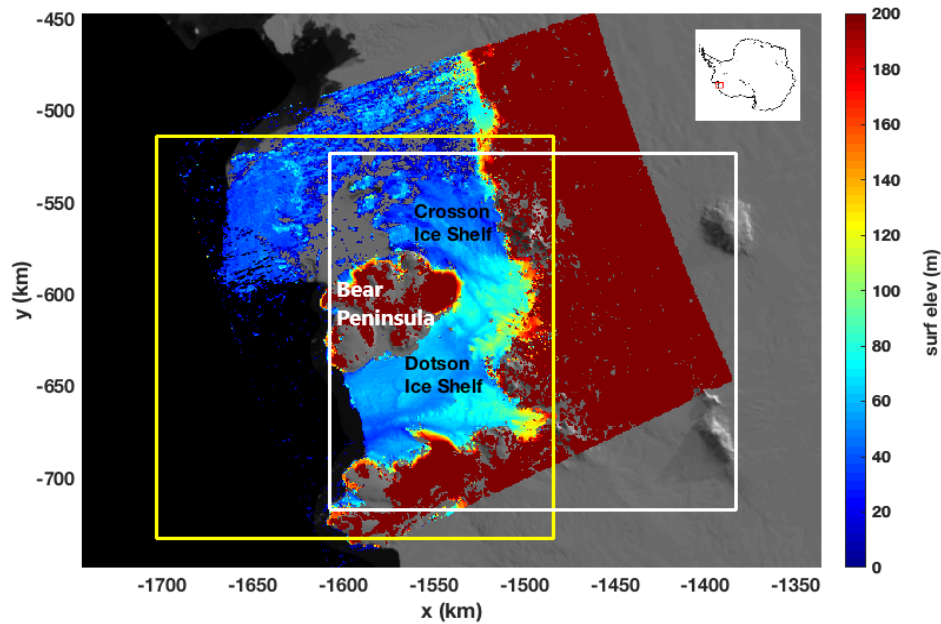


**Figure 1.** Average surface elevation of Dotson and Crosson Ice Shelves, 2011-2015, from CryoSat observations (shading), overlain on MOA imagery. The yellow box indicates the domain of the ocean model used in our study, and the white box that of our ice model. Coordinates are in terms of the stereopolar projection centered at  $71^{\circ}\text{S}$ .

341 In this work, we have utilised an adjoint model to investigate melt sensitivities. De-  
 342 spite its being a linear approximation of nonlinear processes, we would advocate such  
 343 an approach in future investigations of ocean forcing of ice sheets, as it can identify lo-  
 344 cations where understanding of ice-ocean processes is crucial.

### 345 **Acknowledgments**

346 This work was supported by Natural Environment Resources Council grant NE/M003590/1.  
 347 The code used to generate all results, as well as documentation of the models used, is  
 348 available at [mitgcm.org](http://mitgcm.org). All cryosat data is available from <ftp://science-pds.cryosat.esa.int>.  
 349 Ice and ocean modelling output used to produce figures are available as Supplementary  
 350 Material. Additionally DNG is grateful to J DeRydt for helpful conversations in the de-  
 351 velopment of this work.

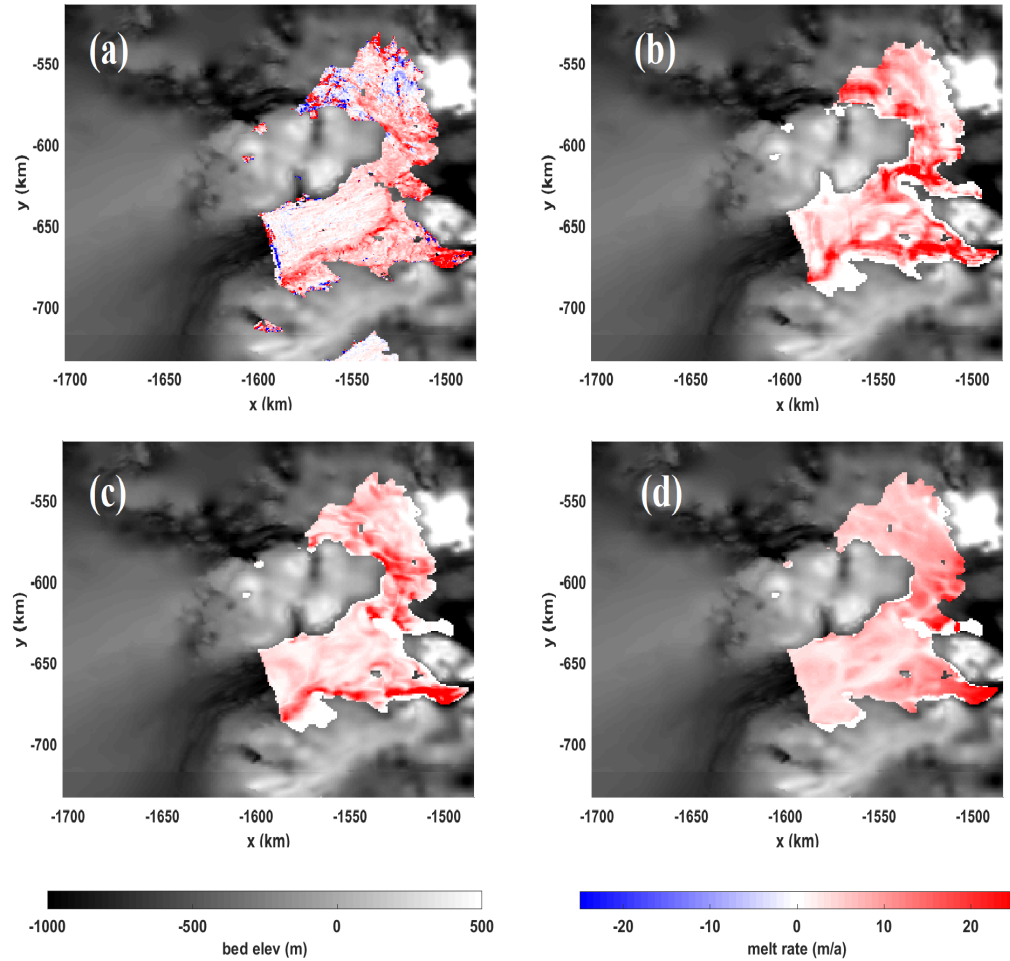


**Figure 2.** (a) Melt rates inferred from CryoSat elevation change using Eq. 1 (color shading), overlain on the Millan bathymetry (B/W) and plotted for the ocean model domain. The Millan dataset does not reach the edge of the domain in the west, and so is replaced by BEDMAP2 in this region. (b) Average melt rate of Model 1 over the same period. (c) Similarly for Model 2. (d) Similarly for Model 3.

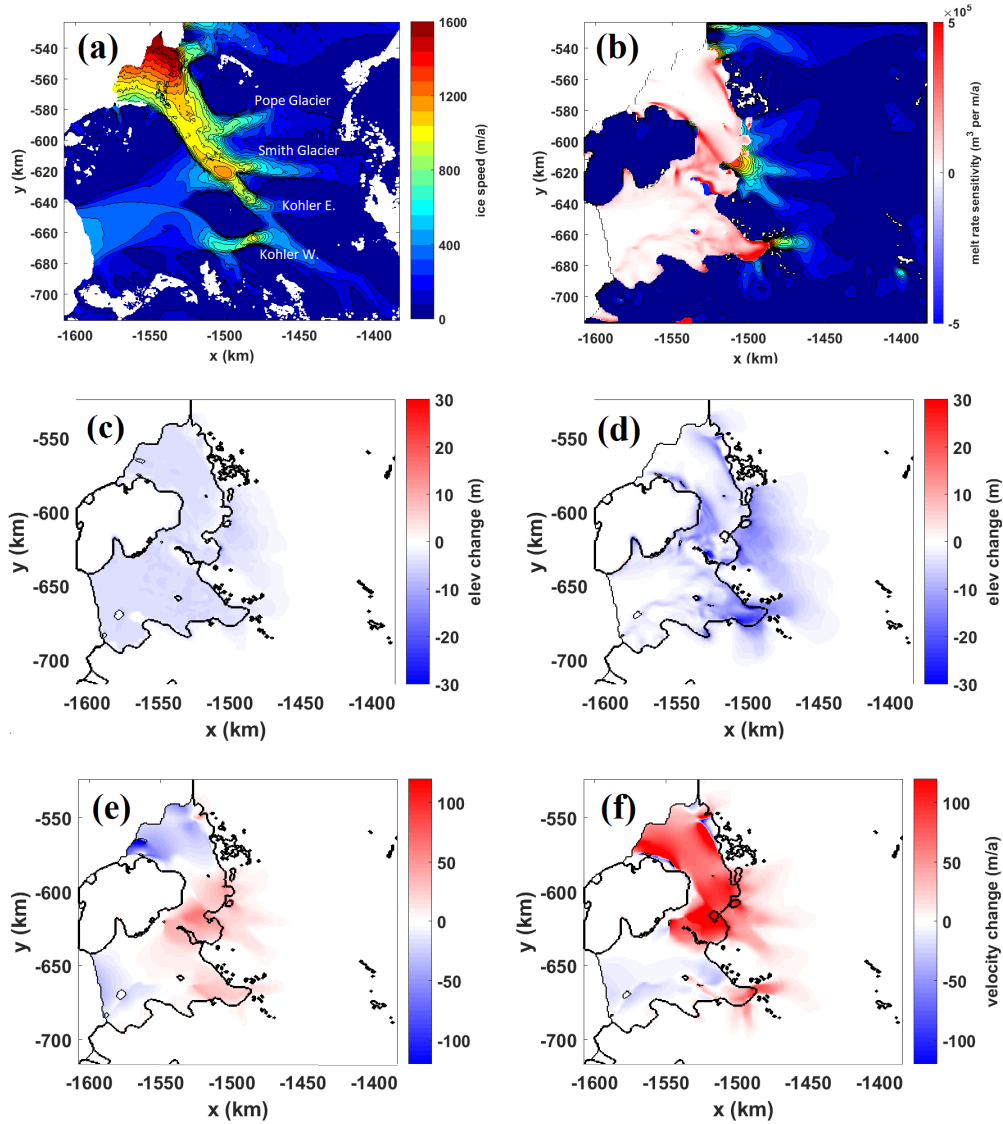


**Figure 3.** (a) MEaSUREs ice speed within ice model domain. (b) Adjoint melt rate sensitivities over the ice shelf (Red/Blue shading) and modelled grounded ice velocity (filled contours). (c) Total modelled surface elevation change in *CONST* ice model simulation, relative to that of *CONTROL*. Note the grounding line location is given by the thick black contour. (d) As in (c) but for *FOCUS* simulation. (e) Change in ice-stream and ice-shelf speed in *CONST* simulation relative to *CONTROL*. Again, the grounding line is denoted by the thick black contour. Difference in velocity is projected onto the direction of velocity in *CONTROL*. (f) as in (e) but for *FOCUS* simulation.



(Obs / model)	Bathy	Draft	Melt Param.	Avg Melt, Crosson (ma <sup>-1</sup> )	Avg Melt, Dotson (ma <sup>-1</sup> )	Avg Melt, Combined (ma <sup>-1</sup> )	Est. VAF Loss (km <sup>3</sup> )
CryoSat	N/A	N/A	N/A	7.15 (5.39)	6.68 (5.70)	6.86 (5.58)	2.4 (-4.0)
Model 1	Millan	Millan	u-dep	7.11	7.80	7.55	N/A
Model 2	Millan	CryoSat	u-dep	6.72	6.43	6.53	-4.2
Model 3	Millan	CryoSat	u-indep	7.42	6.82	7.05	-3.0
Model 4	RTOPO	RTOPO	u-dep	N/A	2.66	2.66	-23

**Table 1.** Table of observed and modelled melt rates and grounded volume response. Melt values in parentheses indicate an alternative method of filtering the observations. The final column represents a linear estimate of VAF loss relative to the *CONTROL* run, calculated via Eq. 3.

**References**

- 352  
353 Arneborg, L., A. K. Wåhlin, G. Björk, B. Liljebladh, and A. H. Orsi, Persistent  
354 inflow of warm water onto the central amundsen shelf, *Nature Geoscience*, *5*,  
355 876–880, doi:10.1038/ngeo1644, 2012.
- 356 Arthern, R., and C. R. Williams, The sensitivity of west antarctica to the sub-  
357 marine melting feedback, *Geophysical Research Letters*, *44*(5), 2352–2359, doi:  
358 10.1002/2017GL072514, 2017.
- 359 Arthern, R. J., D. P. Winebrenner, and D. G. Vaughan, Antarctic snow accu-  
360 mulation mapped using polarization of 4.3-cm wavelength microwave emis-  
361 sion, *Journal of Geophysical Research: Atmospheres*, *111*(D6), D06,107, doi:  
362 10.1029/2004JD005667, 2006.
- 363 Berger, S., R. Drews, V. Helm, S. Sun, and F. Pattyn, Detecting high spatial vari-  
364 ability of ice shelf basal mass balance, roi baudouin ice shelf, antarctica, *The*  
365 *Cryosphere*, *11*(6), 2675–2690, doi:10.5194/tc-11-2675-2017, 2017.
- 366 Borstad, C., A. Khazendar, B. Scheuchl, M. Morlighem, E. Larour, and E. Rig-  
367 not, A constitutive framework for predicting weakening and reduced buttressing  
368 of ice shelves based on observations of the progressive deterioration of the rem-  
369 nant Larsen B Ice Shelf, *Geophysical Research Letters*, *43*(5), 2027–2035, doi:  
370 10.1002/2015GL067365, 2016.
- 371 Brunt, K. M., H. A. Fricker, L. Padman, T. A. Scambos, and S. O’Neel, Mapping  
372 the grounding zone of the ross ice shelf, antarctica, using icesat laser altimetry,  
373 *Annals of Glaciology*, *51*(55), 71–79, doi:10.3189/172756410791392790, 2010.
- 374 Cuffey, K., and W. S. B. Paterson, *The Physics of Glaciers*, 4th ed., Butterworth  
375 Heinemann, Oxford, 2010.
- 376 Dansereau, V., P. Heimbach, and M. Losch, Simulation of subice shelf melt rates  
377 in a general circulation model: Velocity-dependent transfer and the role of  
378 friction, *Journal of Geophysical Research: Oceans*, *119*(3), 1765–1790, doi:  
379 10.1002/2013JC008846, 2014.
- 380 Depoorter, M. A., J. L. Bamber, J. A. Griggs, J. T. M. Lenaerts, S. R. M. Ligten-  
381 berg, M. R. van den Broeke, and G. Moholdt, Calving fluxes and basal melt rates  
382 of Antarctic ice shelves, *Nature*, *502*, 89–92, doi:doi:10.1038/nature12567, 2013.
- 383 Dupont, T. K., and R. Alley, Assessment of the importance of ice-shelf buttressing  
384 to ice-sheet flow, *Geophys. Res. Lett.*, *32*, L04,503, 2005.

- 385 Dutrieux, P., D. G. Vaughan, H. F. J. Corr, A. Jenkins, P. R. Holland, I. Joughin,  
386 and A. H. Fleming, Pine island glacier ice shelf melt distributed at kilometre  
387 scales, *The Cryosphere*, 7(5), 1543–1555, doi:10.5194/tc-7-1543-2013, 2013.
- 388 Dutrieux, P., et al., Strong sensitivity of pine island ice-shelf melting to climatic  
389 variability, *Science*, 343(6167), 174–178, doi:10.1126/science.1244341, 2014.
- 390 Fretwell, P., et al., Bedmap2: improved ice bed, surface and thickness datasets for  
391 Antarctica, *The Cryosphere*, 7(1), 375–393, doi:10.5194/tc-7-375-2013, 2013.
- 392 Fürst, J. J., G. Durand, F. Gillet-Chaulet, N. Merino, L. Tavard, J. Mouginot,  
393 N. Gourmelen, and O. Gagliardini, Assimilation of antarctic velocity observations  
394 provides evidence for uncharted pinning points, *The Cryosphere*, 9(4), 1427–1443,  
395 doi:10.5194/tc-9-1427-2015, 2015.
- 396 Goldberg, D. N., A variationally-derived, depth-integrated approximation to a  
397 higher-order glaciological flow model, *Journal of Glaciology*, 57, 157–170, 2011.
- 398 Goldberg, D. N., and P. Heimbach, Parameter and state estimation with a time-  
399 dependent adjoint marine ice sheet model, *The Cryosphere*, 7(6), 1659–1678,  
400 doi:10.5194/tc-7-1659-2013, 2013.
- 401 Goldberg, D. N., C. M. Little, O. V. Sergienko, A. Gnanadesikan, R. Hallberg, and  
402 M. Oppenheimer, Investigation of land ice-ocean interaction with a fully coupled  
403 ice-ocean model, Part 2: Sensitivity to external forcings, *Journal of Geophysical  
404 Research-Earth Surface*, 117, F02,038, doi:10.1029/2011JF002246, 2012.
- 405 Goldberg, D. N., P. Heimbach, I. Joughin, and B. Smith, Committed retreat of  
406 smith, pope, and kohler glaciers over the next 30 years inferred by transient model  
407 calibration, *The Cryosphere*, 9(6), 2429–2446, doi:10.5194/tc-9-2429-2015, 2015.
- 408 Goldberg, D. N., S. H. K. Narayanan, L. Hascoet, and J. Utke, An optimized  
409 treatment for algorithmic differentiation of an important glaciological fixed-  
410 point problem, *Geoscientific Model Development*, 9(5), 1891–1904, doi:  
411 10.5194/gmd-9-1891-2016, 2016.
- 412 Gourmelen, N., M. Escorihuela, A. Shepherd, L. Foresta, A. Muir, A. Garcia-  
413 Mondjar, M. Roca, S. Baker, and M. Drinkwater, Cryosat-2 swath interferometric  
414 altimetry for mapping ice elevation and elevation change, *Advances in Space Re-  
415 search*, 62(6), 1226 – 1242, doi:https://doi.org/10.1016/j.asr.2017.11.014, 2018.
- 416 Gourmelen, N., et al., Channelized melting drives thinning under a rapidly melt-  
417 ing antarctic ice shelf, *Geophysical Research Letters*, 44(19), 9796–9804, doi:

- 418 10.1002/2017GL074929, 2017.
- 419 Greenbaum, J. S., et al., Ocean access to a cavity beneath Totten Glacier in East  
420 Antarctica, *Nature Geoscience*, *8*, 294–298, doi:<https://doi.org/10.1038/ngeo2388>,  
421 2015.
- 422 Holland, D. M., and A. Jenkins, Modelling thermodynamic ice-ocean interac-  
423 tions at the base of an ice shelf, *J. Phys. Ocean.*, *29*, 1787–1800, doi:[https://doi.org/10.1175/1520-0485\(1999\)029](https://doi.org/10.1175/1520-0485(1999)029), 1999.
- 424
- 425 Jacobs, S., A. Jenkins, H. Hellmer, C. Giulivi, F. Nitsche, B. Huber, and R. Guer-  
426 rero, The Amundsen Sea and the Antarctic Ice Sheet, *Oceanography*, *25*, doi:  
427 <https://doi.org/10.5670/oceanog.2012.90>, 2012.
- 428 Jacobs, S. S., A. Jenkins, C. Giulivi, and P. Dutrieux, Stronger ocean circulation  
429 and increased melting under Pine Island Glacier ice shelf, *Nat. Geosci.*, doi:  
430 10.1038/NCEO1188, 2011.
- 431 Jenkins, A., and C. Doake, Ice-ocean interaction on Ronne Ice Shelf, Antarc-  
432 tica, *Journal of Geophysical Research: Oceans*, *96*(C1), 791–813, doi:10.1029/  
433 90JC01952, 1991.
- 434 Jenkins, A., P. Dutrieux, S. Jacobs, E. J. Steig, H. Gudmundsson, J. Smith, and  
435 K. Heywood, Decadal ocean forcing and antarctic ice sheet response: Lessons from  
436 the amundsen sea, *Oceanography*, *29*, doi:[https://doi.org/10.5670/oceanog.2016.](https://doi.org/10.5670/oceanog.2016.103)  
437 103, 2016.
- 438 Jenkins, A., D. Shoosmith, P. Dutrieux, S. Jacobs, T. W. Kim, S. H. Le, H. K.  
439 Ha, and S. Stammerjohn, West antarctic ice sheet retreat in the amundsen  
440 sea driven by decadal oceanic variability, *Nat. Geoscience*, *11*, 733–738, doi:  
441 <https://doi.org/10.1038/s41561-018-0207-4DO>, 2018.
- 442 Joughin, I., B. E. Smith, and B. Medley, Marine ice sheet collapse potentially un-  
443 der way for the Thwaites Glacier Basin, West Antarctica, *Science*, *344*(6185),  
444 735–738, doi:10.1126/science.1249055, 2014.
- 445 Jourdain, N. C., J.-M. Molines, J. L. Sommer, P. Mathiot, J. Chanut,  
446 C. de Lavergne, and G. Madec, Simulating or prescribing the influence of  
447 tides on the amundsen sea ice shelves, *Ocean Modelling*, *133*, 44 – 55, doi:  
448 <https://doi.org/10.1016/j.ocemod.2018.11.001>, 2019.
- 449 Khazendar, A., E. Rignot, D. Schroeder, H. Seroussi, M. Schodlok, B. Scheuchl,  
450 J. Mouginot, T. Sutterley, and I. Velicogna, Rapid submarine ice melting in the

- 451 grounding zones of ice shelves in West Antarctica, *Nature Communications*, 7,  
452 13,243, doi:<http://dx.doi.org/10.1038/ncomms13243>, 2016.
- 453 Kimura, S., et al., Oceanographic controls on the variability of ice shelf basal  
454 melting and circulation of glacial meltwater in the Amundsen Sea embayment,  
455 Antarctica, *Journal of Geophysical Research: Oceans*, 122(12), 10,131–10,155,  
456 doi:10.1002/2017JC012926, 2017.
- 457 Ligtenberg, S. R. M., P. Kuipers Munneke, and M. R. van den Broeke, Present and  
458 future variations in Antarctic firn air content, *The Cryosphere*, 8(5), 1711–1723,  
459 doi:10.5194/tc-8-1711-2014, 2014.
- 460 Lilien, D. A., I. Joughin, B. Smith, and D. E. Shean, Changes in flow of Ross and  
461 Dotson ice shelves, West Antarctica, in response to elevated melt, *The Cryosphere*,  
462 12(4), 1415–1431, doi:10.5194/tc-12-1415-2018, 2018.
- 463 Little, C. M., A. Gnanadesikan, and M. Oppenheimer, How ice shelf morphology  
464 controls basal melting, *Journal of Geophysical Research*, 114, C12,007, 2009.
- 465 Losch, M., Modeling ice shelf cavities in a z coordinate ocean general circula-  
466 tion model, *Journal of Geophysical Research: Oceans*, 113(C8), n/a–n/a, doi:  
467 10.1029/2007JC004368, 2008.
- 468 MacAyeal, D. R., The basal stress distribution of Ice Stream E, Antarctica, inferred  
469 by control methods, *Journal of Geophysical Research*, 97, 595–603, 1992.
- 470 Marshall, J., C. Hill, L. Perelman, and A. Adcroft, Hydrostatic, quasi-hydrostatic,  
471 and nonhydrostatic ocean modeling, *Journal of Geophysical Research: Oceans*,  
472 102(C3), 5733–5752, doi:10.1029/96JC02776, 1997.
- 473 McMillan, M., A. Shepherd, A. Sundal, K. Briggs, A. Muir, A. Ridout, A. Hogg,  
474 and D. Wingham, Increased ice losses from Antarctica detected by CryoSat-2,  
475 *Geophysical Research Letters*, 41(11), 3899–3905, doi:10.1002/2014GL060111,  
476 2014a.
- 477 McMillan, M., et al., Rapid dynamic activation of a marine-based arctic ice cap,  
478 *Geophysical Research Letters*, 41(24), 8902–8909, doi:10.1002/2014GL062255,  
479 2014b.
- 480 Miles, T., S. H. Lee, A. Wåhlin, H. K. Ha, T. W. Kim, K. M. Assmann, and  
481 O. Schofield, Glider observations of the Dotson Ice Shelf outflow, *Deep Sea  
482 Research Part II: Topical Studies in Oceanography*, 123, 16 – 29, doi:<https://doi.org/10.1016/j.dsr2.2015.08.008>, 2016.

- 484 Millan, R., E. Rignot, V. Bernier, M. Morlighem, and P. Dutrieux, Bathymetry of  
485 the Amundsen Sea Embayment sector of West Antarctica from Operation Ice-  
486 Bridge gravity and other data, *Geophysical Research Letters*, *44*(3), 1360–1368,  
487 doi:10.1002/2016GL072071, 2017.
- 488 Mouginot, J., E. Rignot, and B. Scheuchl, Sustained increase in ice discharge from  
489 the amundsen sea embayment, west antarctica, from 1973 to 2013, *Geophysical*  
490 *Research Letters*, *41*(5), 1576–1584, doi:10.1002/2013GL059069, 2014.
- 491 Nakayama, Y., D. Menemenlis, M. Schodlok, and E. Rignot, Amundsen and belling-  
492 shausen seas simulation with optimized ocean, sea ice, and thermodynamic ice  
493 shelf model parameters, *Journal of Geophysical Research: Oceans*, *122*(8), 6180–  
494 6195, doi:10.1002/2016JC012538, 2017.
- 495 Paolo, F. S., H. A. Fricker, and L. Padman, Volume loss from Antarctic ice shelves is  
496 accelerating, *Science*, *348*(6232), 327–331, doi:10.1126/science.aaa0940, 2015.
- 497 Pattyn, F., et al., Grounding-line migration in plan-view marine ice-sheet models:  
498 results of the ice2sea mismip3d intercomparison, *Journal of Glaciology*, *59*(215),  
499 410?422, doi:10.3189/2013JoG12J129, 2013.
- 500 Payne, A. J., P. R. Holland, A. Shepherd, I. C. Rutt, A. Jenkins, and I. Joughin,  
501 Numerical modeling of ocean-ice interactions under Pine Island Bay’s ice shelf,  
502 *Journal of Geophysical Research-Oceans*, *112*, C10,019, 2007.
- 503 Petty, A. A., D. L. Feltham, and P. R. Holland, Impact of Atmospheric Forcing on  
504 Antarctic Continental Shelf Water Masses, *Journal of Physical Oceanography*,  
505 *43*(5), 920–940, doi:10.1175/JPO-D-12-0172.1, 2013.
- 506 Pritchard, H. D., S. R. M. Ligtenberg, H. A. Fricker, D. G. Vaughan, M. R. van den  
507 Broeke, and L. Padman, Antarctic ice-sheet loss driven by basal melting of ice  
508 shelves, *Nature*, *484*, 502–505, doi:doi:10.1038/nature10968, 2012.
- 509 Randall-Goodwin, E., et al., Freshwater distributions and water mass struc-  
510 ture in the Amundsen Sea Polynya region, Antarctica, *Elementa*, *5*, 65, doi:  
511 <http://doi.org/10.12952/journal.elementa.000065>, 2015.
- 512 Reese, R., G. H. Gudmundsson, A. Levermann, and R. Winkelmann, The far  
513 reach of ice-shelf thinning in antarctica, *Nature Climate Change*, *8*, 53–57, doi:  
514 <https://doi.org/10.1038/s41558-017-0020-x>, 2018.
- 515 Rignot, E., J. Mouginot, and B. Scheuchl, Ice flow of the Antarctic Ice Sheet, *Sci-*  
516 *ence*, *333*(6048), 1427–1430, doi:10.1126/science.1208336, 2011.

- 517 Rignot, E., S. Jacobs, J. Mouginot, and B. Scheuchl, Ice-Shelf Melting Around  
518 Antarctica, *Science*, *341*(6143), 266–270, doi:10.1126/science.1235798, 2013.
- 519 Rignot, E., J. Mouginot, M. Morlighem, H. Seroussi, and B. Scheuchl, Widespread,  
520 rapid grounding line retreat of Pine Island, Thwaites, Smith and Kohler glaciers,  
521 West Antarctica from 1992 to 2011, *Geophysical Research Letters*, *41*, 3502–3509,  
522 doi:10.1002/2014GL060140, 2014.
- 523 Robertson, R., Tidally induced increases in melting of Amundsen Sea ice  
524 shelves, *Journal of Geophysical Research: Oceans*, *118*(6), 3138–3145, doi:  
525 10.1002/jgrc.20236, 2013.
- 526 Scheuchl, B., J. Mouginot, E. Rignot, M. Morlighem, and A. Khazendar, Ground-  
527 ing line retreat of Pope, Smith, and Kohler Glaciers, West Antarctica, measured  
528 with Sentinel-1a radar interferometry data, *Geophysical Research Letters*, *43*(16),  
529 8572–8579, doi:10.1002/2016GL069287, 2016.
- 530 Schodlok, M. P., D. Menemenlis, E. Rignot, and M. Studinger, Sensitivity of the ice-  
531 shelf/ocean system to the sub-ice-shelf cavity shape measured by nasa icebridge  
532 in pine island glacier, west antarctica, *Annals of Glaciology*, *53*(60), 156?162,  
533 doi:10.3189/2012AoG60A073, 2012.
- 534 Seroussi, H., Y. Nakayama, E. Larour, D. Menemenlis, M. Morlighem, E. Rignot,  
535 and A. Khazendar, Continued retreat of thwaites glacier, west antarctica, con-  
536 trolled by bed topography and ocean circulation, *Geophysical Research Letters*,  
537 pp. n/a–n/a, doi:10.1002/2017GL072910, 2017.
- 538 Shepherd, A., D. J. Wingham, and J. Mansley, Inland thinning of the Amund-  
539 sen Sea sector, West Antarctica, *Geophys. Res. Lett.*, *29*, L1364, doi:10.1029/  
540 2001GL014183, 2002.
- 541 Shepherd, A., D. J. Wingham, and E. Rignot, Warm ocean is eroding West Antarc-  
542 tic Ice Sheet, *Geophys. Res. Lett.*, *31*, L23,402, 2004.
- 543 Smith, B. E., N. Gourmelen, A. Huth, and I. Joughin, Connected subglacial lake  
544 drainage beneath thwaites glacier, west antarctica, *The Cryosphere*, *11*(1), 451–  
545 467, doi:10.5194/tc-11-451-2017, 2017.
- 546 Snow, K., D. N. Goldberg, P. R. Holland, J. R. Jordan, R. J. Arthern, and A. Jenk-  
547 ins, The response of ice sheets to climate variability, *Geophysical Research Letters*,  
548 *44*(23), 11,878–11,885, doi:10.1002/2017GL075745, 2017.

- 549 St-Laurent, P., J. M. Klinck, and M. S. Dinniman, Impact of local winter cooling  
550 on the melt of Pine Island Glacier, Antarctica, *Journal of Geophysical Research:  
551 Oceans*, *120*(10), 6718–6732, doi:10.1002/2015JC010709, 2015.
- 552 Thomas, R. H., The dynamics of marine ice sheets, *Journal of Glaciology*, *24*, 167–  
553 177, 1979.
- 554 Timmermann, R., et al., A consistent data set of antarctic ice sheet topography, cav-  
555 ity geometry, and global bathymetry, *Earth System Science Data*, *2*(2), 261–273,  
556 doi:10.5194/essd-2-261-2010, 2010.
- 557 Utke, J., U. Naumann, M. Fagan, N. Tallent, M. Strout, P. Heimbach, C. Hill,  
558 D. Ozyurt, and C. Wunsch, OpenAD/F: A modular open source tool for au-  
559 tomatic differentiation of Fortran codes, *ACM Transactions on Mathematical  
560 Software*, *34*, 2008.
- 561 van Wessem, J. M., et al., The modelled surface mass balance of the antarctic  
562 peninsula at 5.5 km horizontal resolution, *The Cryosphere*, *10*(1), 271–285, doi:  
563 10.5194/tc-10-271-2016, 2016.
- 564 Walker, D. P., A. Jenkins, K. Assmann, D. Shoosmith, and M. Brandon, Oceano-  
565 graphic observations at the shelf break of the Amundsen Sea, Antarctica, *Journal  
566 of Geophysical Research: Oceans*, *118*(6), 2906–2918, doi:10.1002/jgrc.20212, 2013.